

Quantum size effects and optical transitions in topological-insulator nanostructures

Ulrich Zuelicke

*School of Chemical and Physical Sciences, Victoria
University of Wellington, New Zealand*

in collaboration with:

L Gioia *U of Waterloo & Victoria U WLG*

M Christie, M Governale, M Kotulla, A Sneyd *Victoria U WLG*

R Winkler *Northern Illinois U & Argonne Nat'l Lab*



DODD-WALLS CENTRE
for Photonic and Quantum Technologies



Outline

- Introduction & Motivation
 - topological insulators: **inverted bulk band structure**
 - Dirac-like charge carriers: **BHZ model Hamiltonian**
- Quantum size effects in topological-insulator nanostructures: **quantum wells/rings/nanoparticles**
 - fate of topological (sub-)bands & surface states
 - observable consequences: gap oscillations (**2D wells**), conductance oscillations (**1D rings**), optical selection rules & transition probabilities (**0D nanoparticles**)
- Conclusions

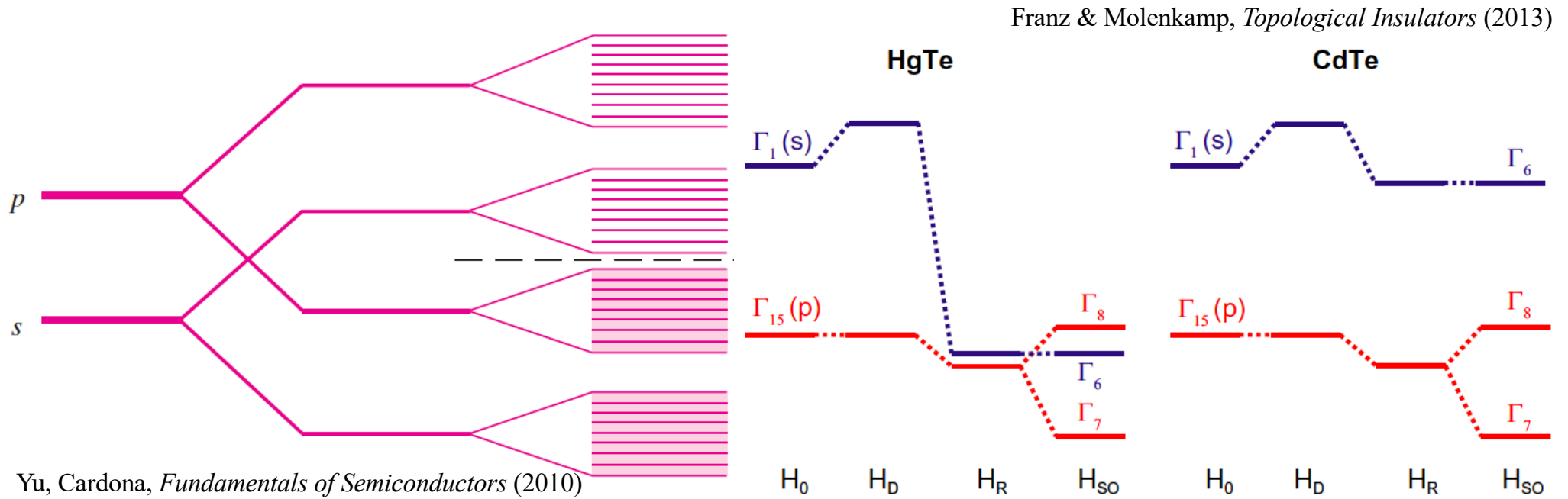


Introduction & Motivation



Topological insulators: Bulk band inversion

- atomic levels broaden into **bands** in solid material
 - (anti-)bonding levels → (conduction) valence bands
- in some materials, relativistic effects reverse order of bonding/anti-bonding bands: **band inversion**

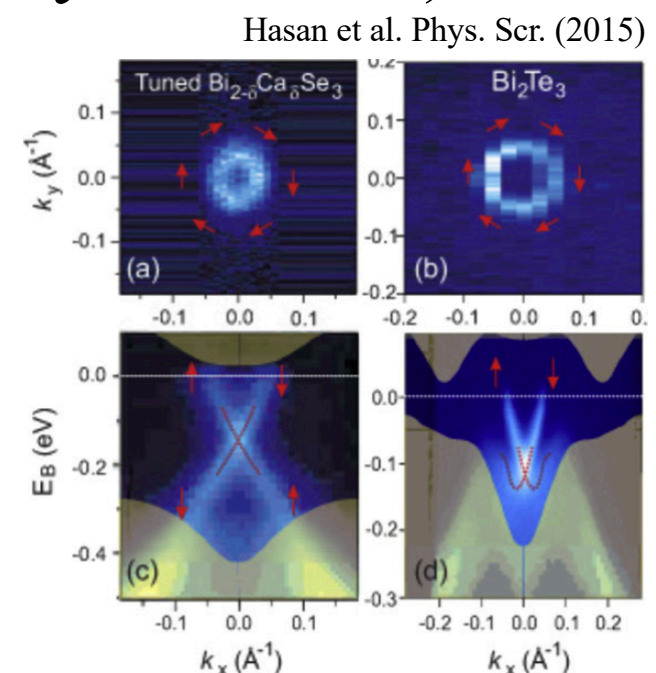
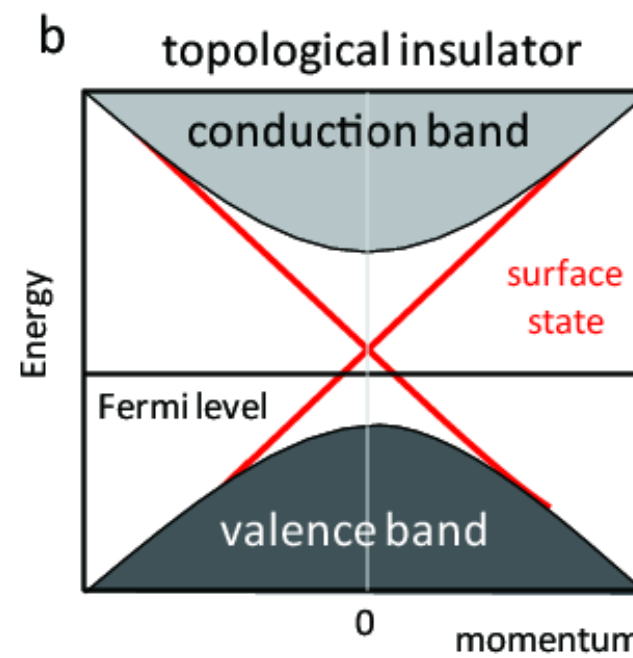
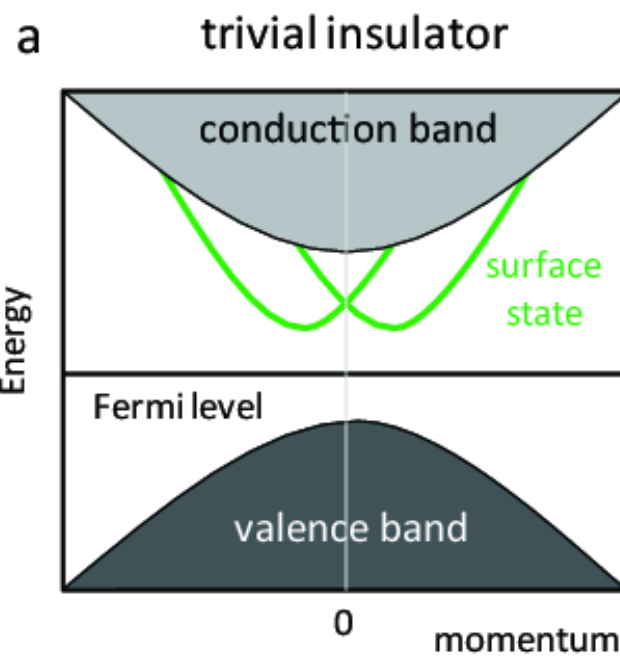


Yu, Cardona, *Fundamentals of Semiconductors* (2010)



Ordinary vs. topological insulator

- closing of gap required to go from ordinary to the inverted situation: **topologically distinct systems!**
- gapless states exist **at the surface** of a topological material (= interface with an ordinary material!)



Size quantization counteracts band inversion

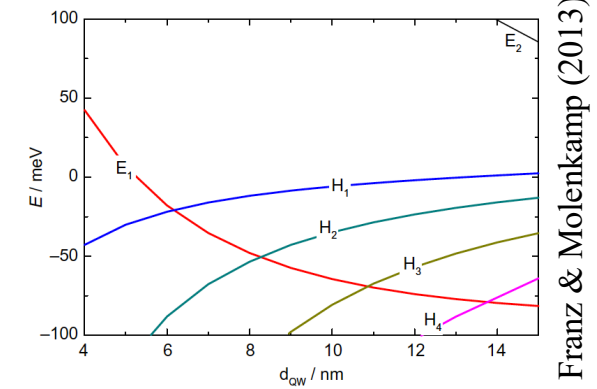
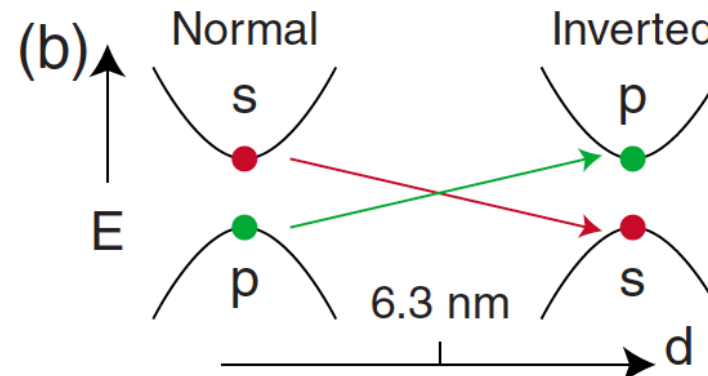
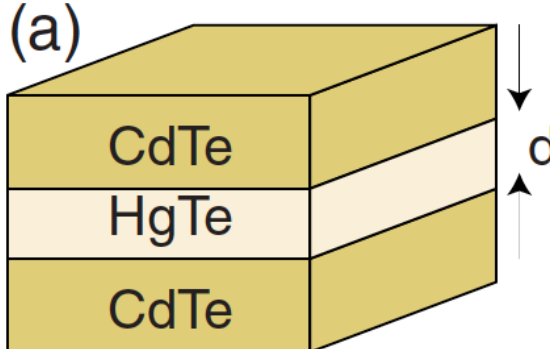
- quantum **bound-state energy adds to bulk band edge**: new (quantum-well) sub-bands

$$\frac{p_x^2 + p_y^2}{2m} + \frac{\Delta_0}{2} + \frac{p_z^2}{2m} + V(z) \longrightarrow \frac{p_x^2 + p_y^2}{2m} + \frac{\Delta_0}{2} + E_n$$

- HgTe quantum well: bulk gap $\Delta_0 < 0$; adjust **well width d** to tune btw. normal & inverted regimes

Bernevig, Hughes & Zhang, Science (2006); König et al., Science (2007)

Hasan & Kane, RMP (2010)



Franz & Molenkamp (2013)

$\mathbf{k} \cdot \mathbf{p}$ theory for Dirac-like charge carriers

- topological insulators generally host **two-flavour Dirac quasiparticles** (pseudospin τ & real spin σ)

$$H = \epsilon(\mathbf{k}) \mathbb{1}_{4 \times 4} + \begin{pmatrix} \frac{\Delta(\mathbf{k})}{2} & \gamma k_- & 0 & \gamma' k_z \\ \gamma k_+ & -\frac{\Delta(\mathbf{k})}{2} & -\gamma' k_z & 0 \\ 0 & -\gamma' k_z & \frac{\Delta(\mathbf{k})}{2} & \gamma k_+ \\ \gamma' k_z & 0 & \gamma k_- & -\frac{\Delta(\mathbf{k})}{2} \end{pmatrix}$$

- includes **2D/3D motion, particle-hole asymmetry**

BHZ, Science (2006); Liu et al., Phys. Rev. B (2010); Brems et al., New J. Phys. (2018)



Confining Dirac-like quasiparticles

- two possibilities: use a **scalar** or a **vector** potential
Greiner, *Relativistic Quantum Mechanics* (1990); Alberto et al., Eur. J. Phys (1996)
 - vector potential models **electrostatic** (e.g. gate-defined) confinement, is not entirely confining (Klein paradox!)
 - scalar potential actually models a **finite materials size**
- adopt **scalar** (i.e., mass-confinement) **potential!**
 - hard-wall, or parabolic, etc. functional form for $V(\mathbf{r})$

$$\mathcal{H} = [\epsilon(\mathbf{k}) + U(\mathbf{r})] \mathbb{1}_{4 \times 4} + \begin{pmatrix} \frac{\Delta(\mathbf{k})}{2} + V(\mathbf{r}) & \gamma k_- & 0 & \gamma' k_z \\ \gamma k_+ & -\frac{\Delta(\mathbf{k})}{2} - V(\mathbf{r}) & -\gamma' k_z & 0 \\ 0 & -\gamma' k_z & \frac{\Delta(\mathbf{k})}{2} + V(\mathbf{r}) & \gamma k_+ \\ \gamma' k_z & 0 & \gamma k_- & -\frac{\Delta(\mathbf{k})}{2} - V(\mathbf{r}) \end{pmatrix}$$

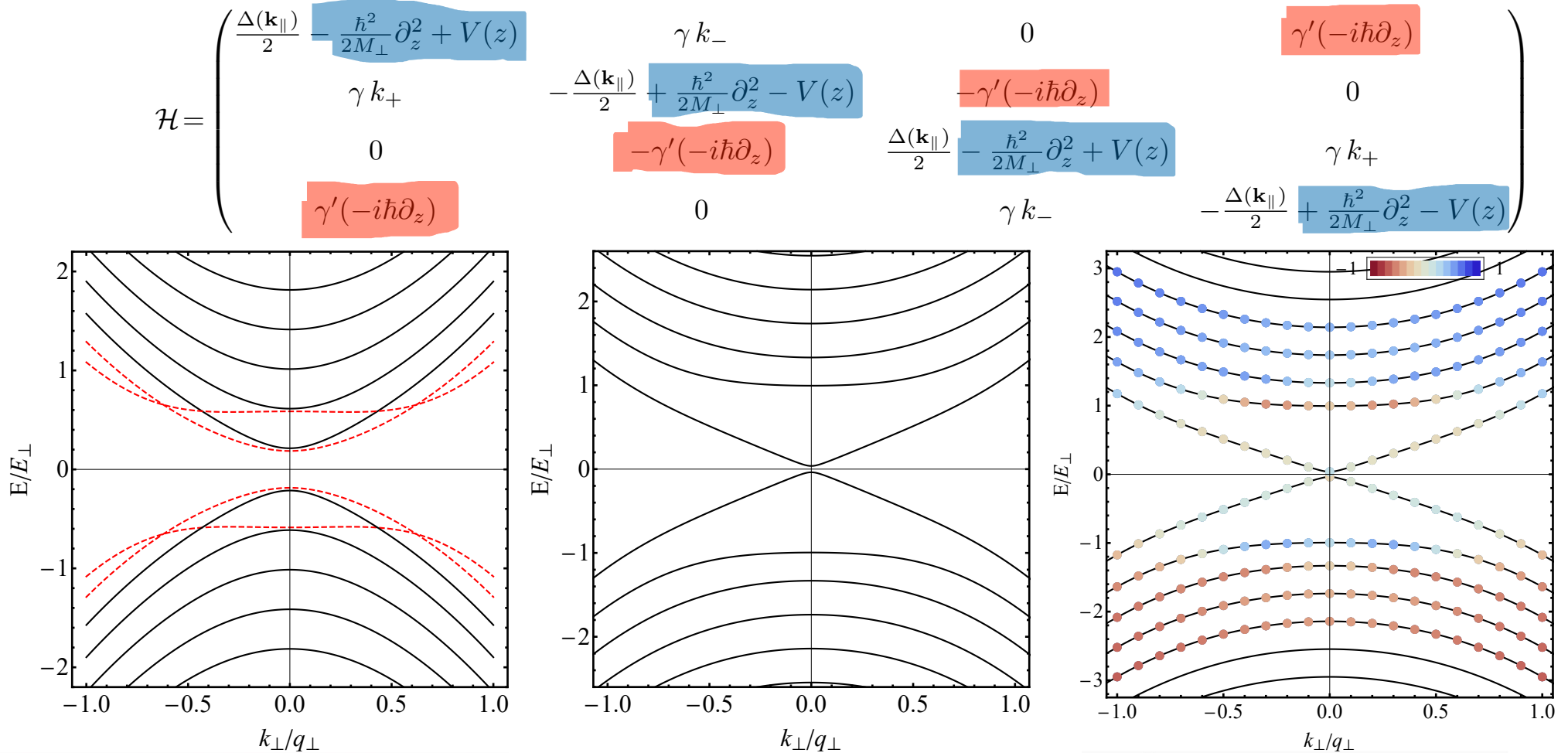


Quasi-2D confinement: Gap oscillations in Bi_2Se_3 -type topological-insulator quantum wells



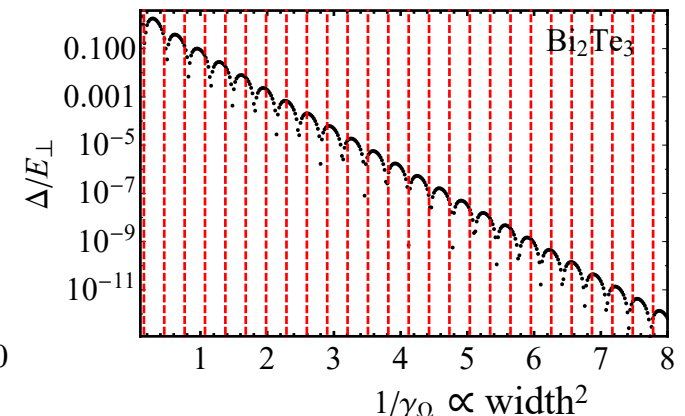
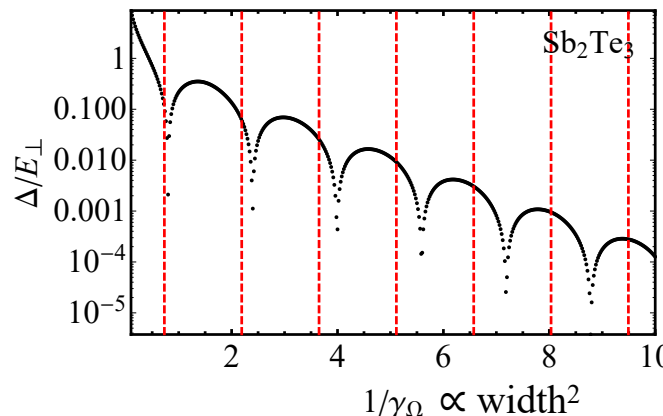
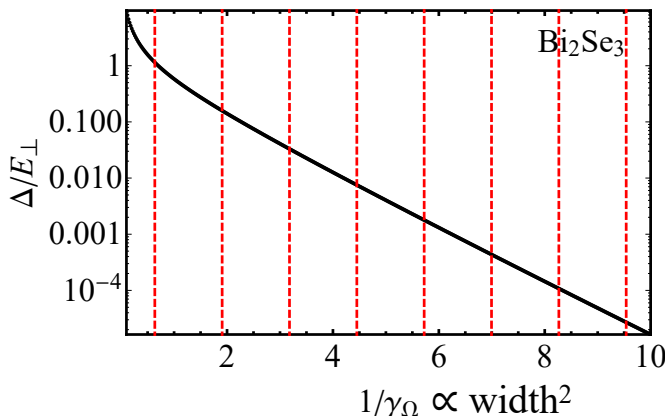
Size-quantized subbands vs. surface states

- interplay of band-edge renormalisation & mixing

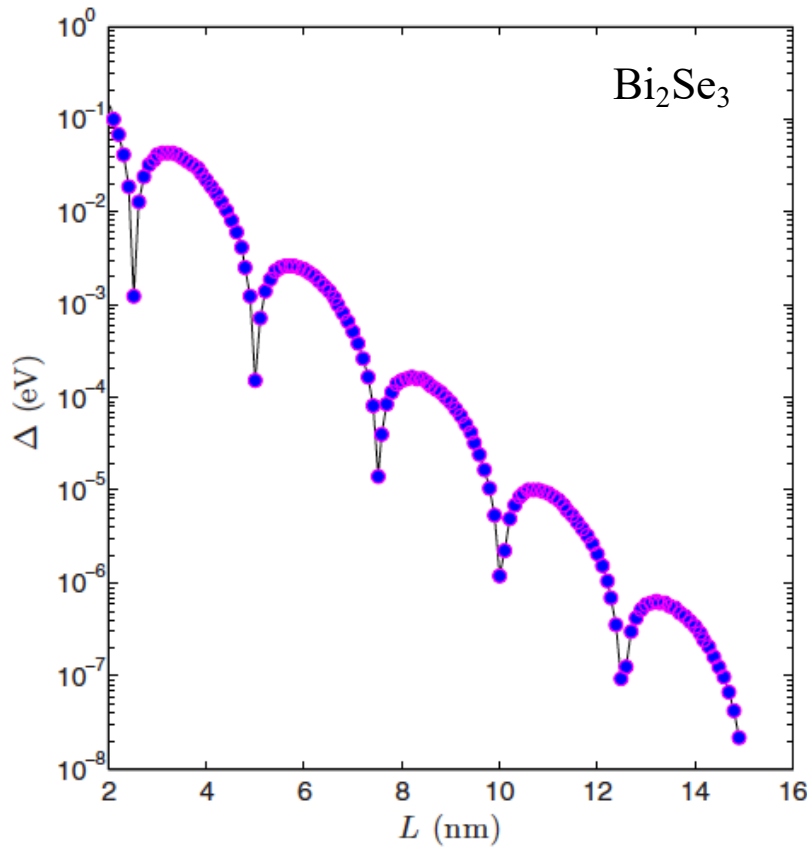


Material-dependent stability of surface states

- Bi₂Se₃-type materials show variety of behavior
 - Bi₂Se₃ maintains 3D topological-insulator features until band inversion is fully destroyed by confinement
 - Sb₂Te₃ has “clean” 2D topological transition similar to that exhibited by HgTe/CdTe quantum well
 - Bi₂Te₃ remains inverted even at smallest layer width

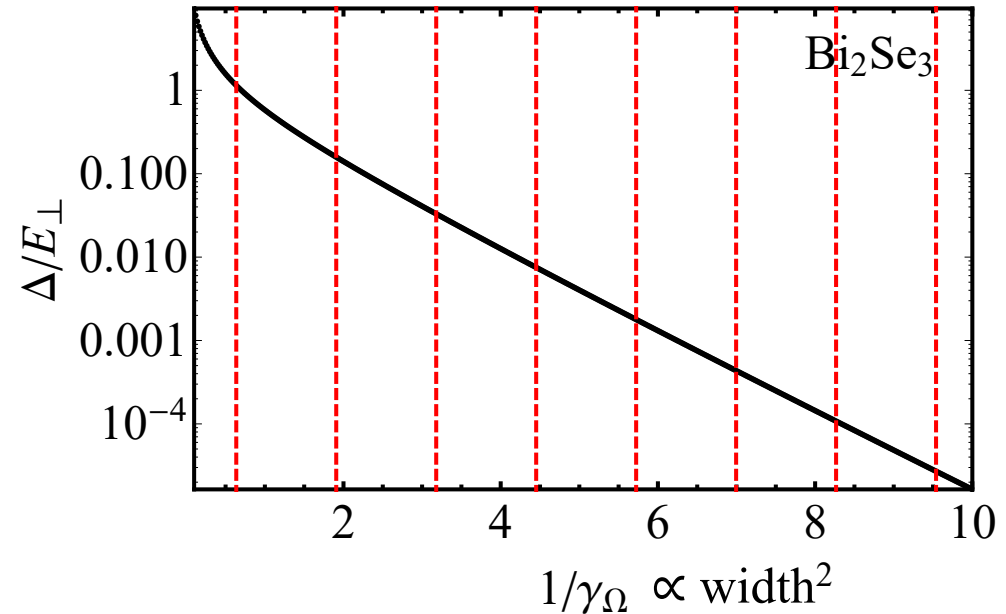


Sensitivity to bulk-bandstructure parameters



Linder et al., Phys. Rev. B (2009)

[band-structure parameters from
Zhang et al., Nat. Phys. (2009)]



Kotulla & UZ, New J. Phys. (2017)

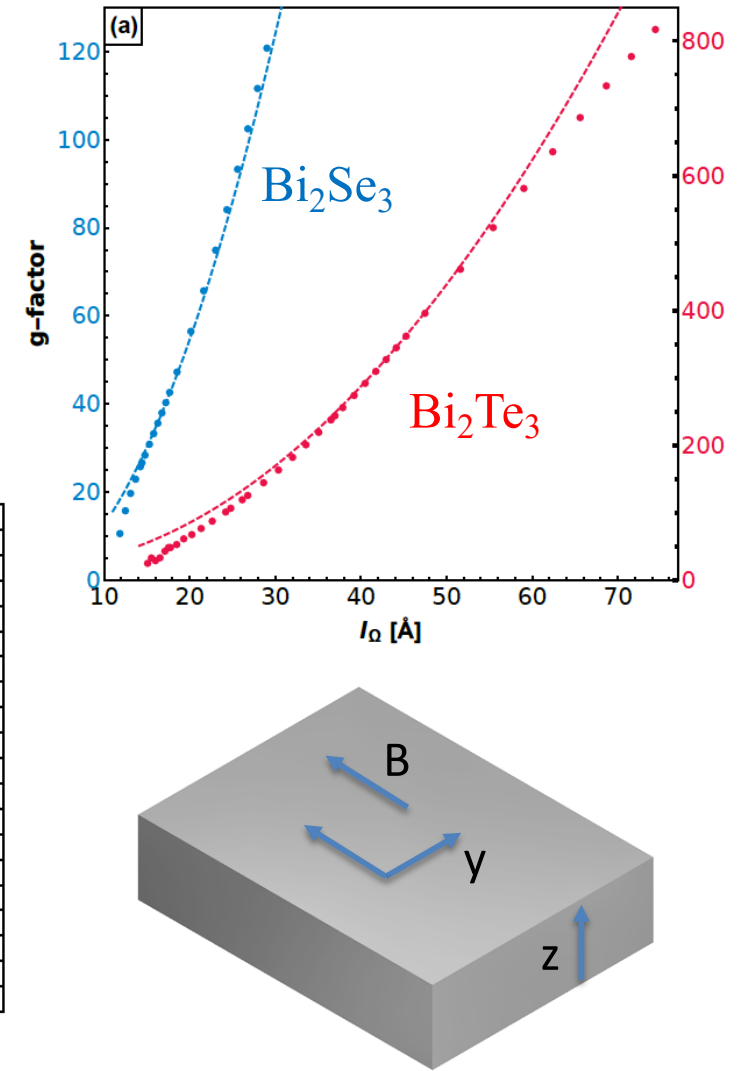
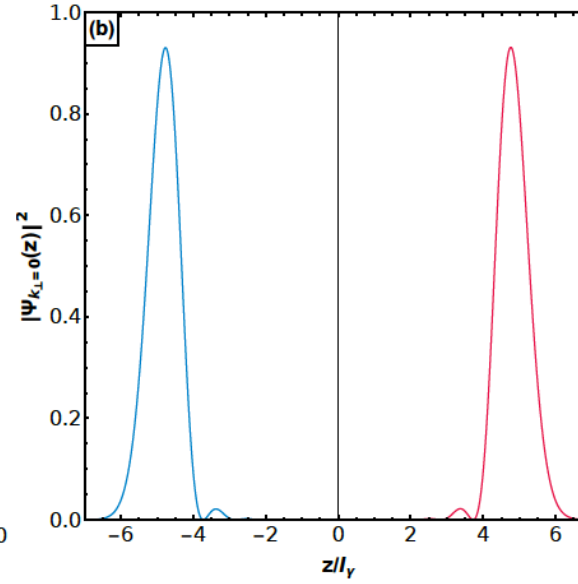
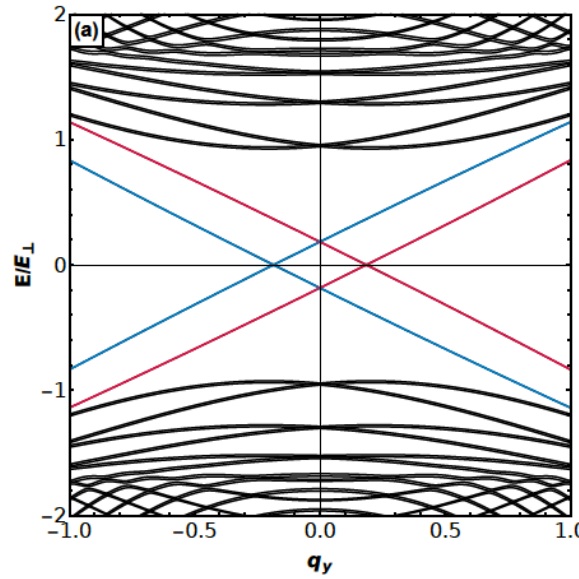
[band-structure parameters from
Nechaev & Krasovskii, PRB (2016)]



In-plane B: Giant surface-state Zeeman splitting

- energy splitting due to in-plane magnetic field **much larger for surface states** than higher bands
 - large effective *g*-factor

Kotulla, PhD thesis (2019)



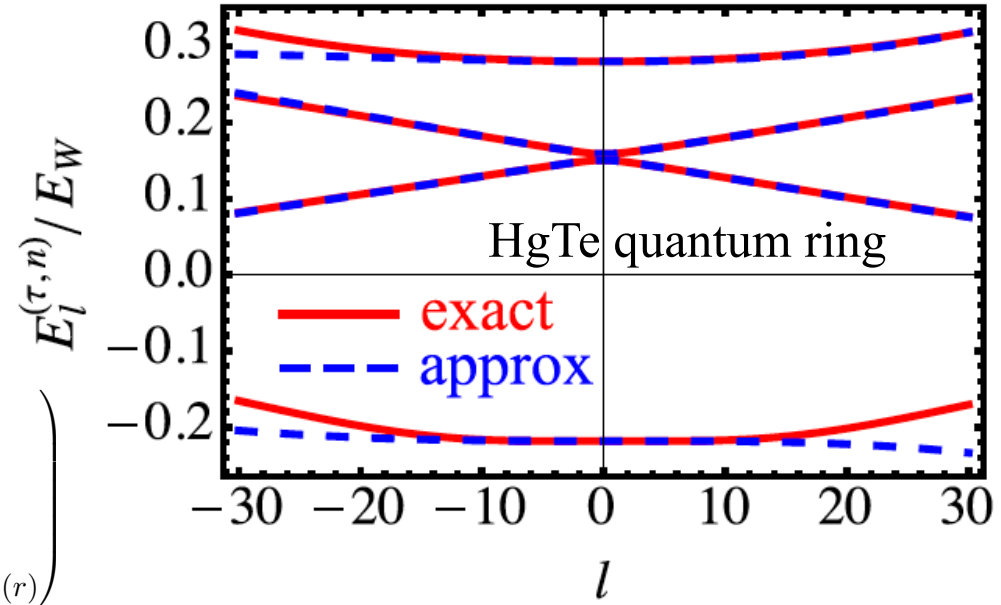
Quasi-1D confinement: Conductance oscillations in quantum-ring structures



2D Dirac-like electrons in quantum rings

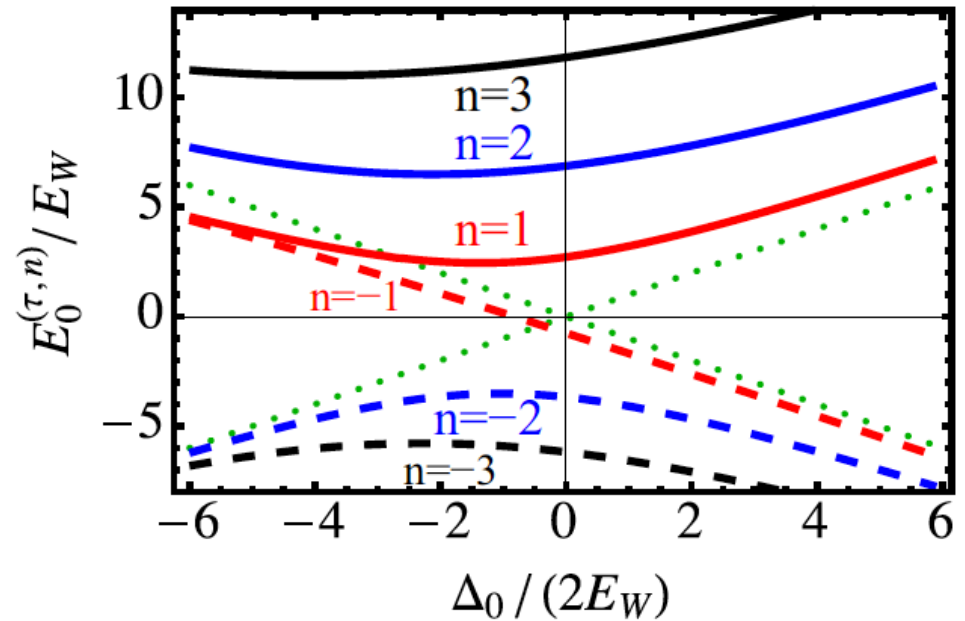
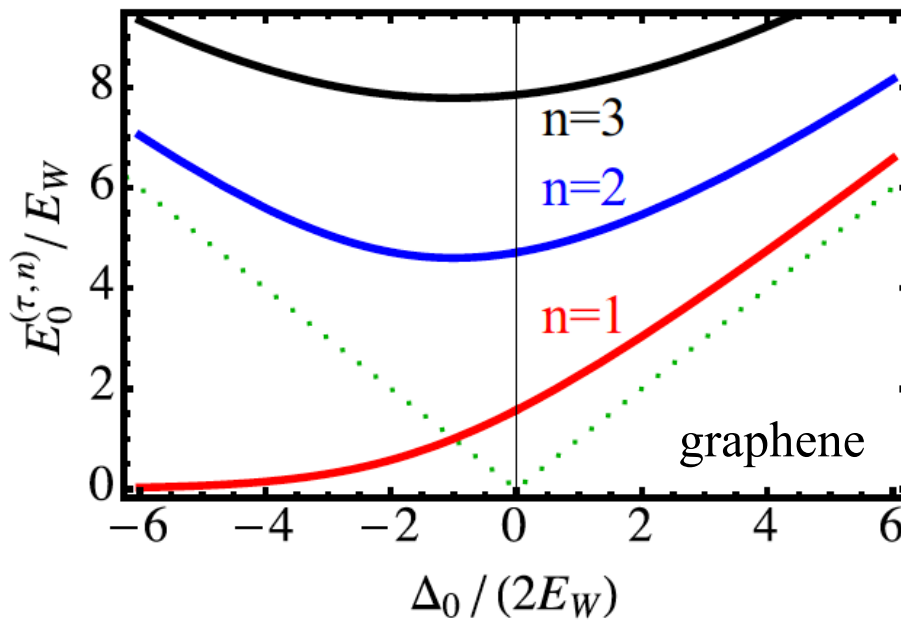
- realizable, e.g., in graphene, HgTe quantum wells
Recher et al., Phys. Rev. B (2007); Michetti & Recher, Phys. Rev. B (2011)
– generically **broken valley/real spin-reversal symmetry**
- can obtain **most general effective quasi-1D Dirac Hamiltonian** for ring subbands Gioia, UZ, et al., PRB (2018)

$$\mathcal{H} = \epsilon(\mathbf{k}) \mathbb{1}_{4 \times 4} + \begin{pmatrix} \frac{\Delta(\mathbf{k})}{2} + V(r) & \gamma k_- & 0 & 0 \\ \gamma k_+ & -\frac{\Delta(\mathbf{k})}{2} - V(r) & 0 & 0 \\ 0 & 0 & \frac{\Delta(\mathbf{k})}{2} + V(r) & \gamma k_+ \\ 0 & 0 & \gamma k_- & -\frac{\Delta(\mathbf{k})}{2} - V(r) \end{pmatrix}$$



Topological regime: Effect of band inversion

- lowest quasi-1D subband energy is below the 2D-bulk band edge if $-\Delta_0/2 \lesssim E_W = \gamma/W$ (W : ring width)

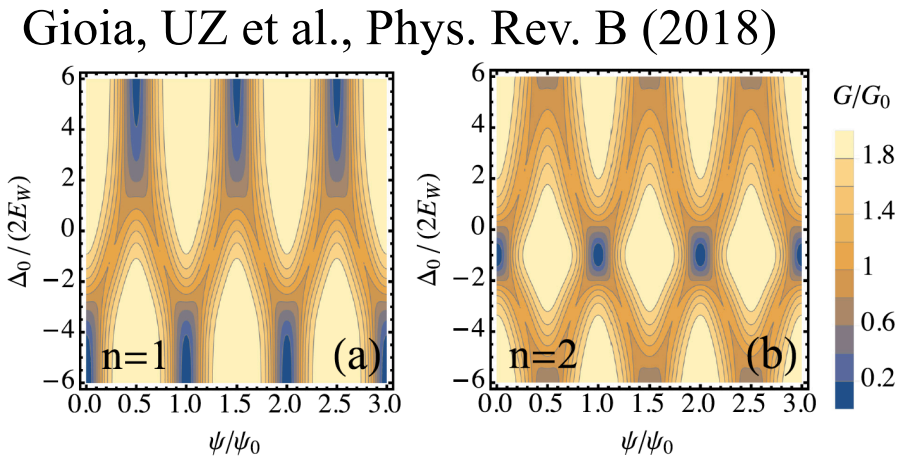
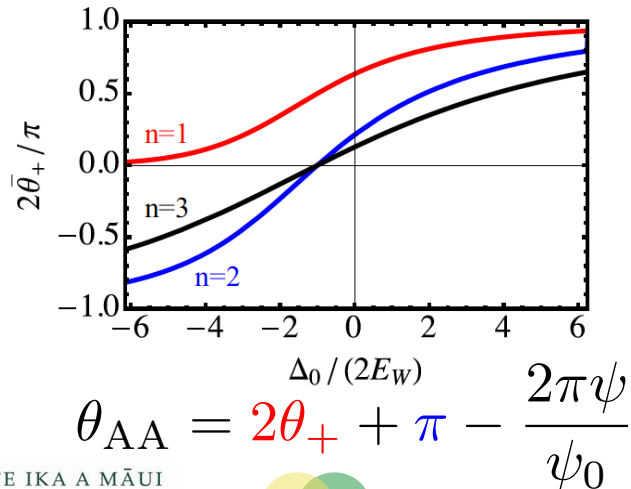
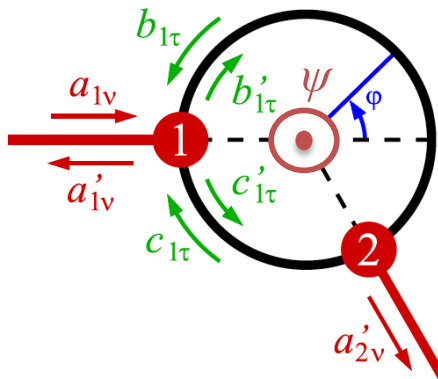


$$\mathcal{H} = \epsilon(\mathbf{k}) \mathbb{1}_{4 \times 4} + \begin{pmatrix} \frac{\Delta(\mathbf{k})}{2} + V(r) & \gamma k_- & 0 & 0 \\ \gamma k_+ & -\frac{\Delta(\mathbf{k})}{2} - V(r) & 0 & 0 \\ 0 & 0 & \frac{\Delta(\mathbf{k})}{2} + V(r) & \gamma k_+ \\ 0 & 0 & \gamma k_- & -\frac{\Delta(\mathbf{k})}{2} - V(r) \end{pmatrix}$$



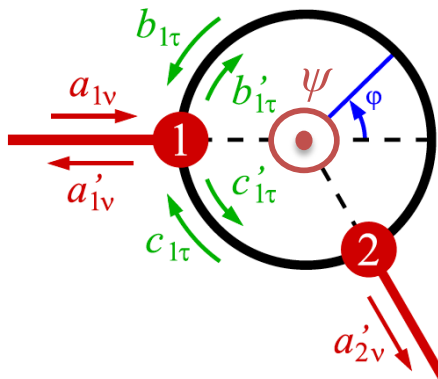
Dirac-ring conductance oscillations

- interference contribution to conductance tuned by enclosed **magnetic flux ψ** Büttiker et al., Phys. Rev. A (1984)
- geometric (**Aharonov-Anandan**) phase revealed in ring-conductance oscillations Frustaglia & Richter, PRB (2004)
- Dirac ring: AA phase **confinement-dependent** and reflects **topological property** of lowest subband



Valley(or spin)-dependent transport

- robust tunable conductance polarization
- engineer based on fully general analytic results!



$$T_\tau(\chi, \tilde{\chi}_\tau, \theta_{AA}^{(\tau)}) = \frac{4\varepsilon_{1\tau}\varepsilon_{2\tau} [\cos^2 \chi \sin^2 \tilde{\chi}_\tau \cos^2 (\theta_{AA}^{(\tau)}/2) + \sin^2 \chi \cos^2 \tilde{\chi}_\tau \sin^2 (\theta_{AA}^{(\tau)}/2)]}{|\kappa_{1\tau}||\kappa_{2\tau}| e^{i(\varrho_{1\tau}+\varrho_{2\tau})} \cos(2\chi) + |\lambda_{1\tau}||\lambda_{2\tau}| e^{-i(\varrho_{1\tau}+\varrho_{2\tau})} \cos \theta_{AA}^{(\tau)} - F_\tau(\omega_{1\tau} + \omega_{2\tau}, \phi_{1\tau} + \phi_{2\tau}, 2\tilde{\chi}_\tau)|^2}$$

where

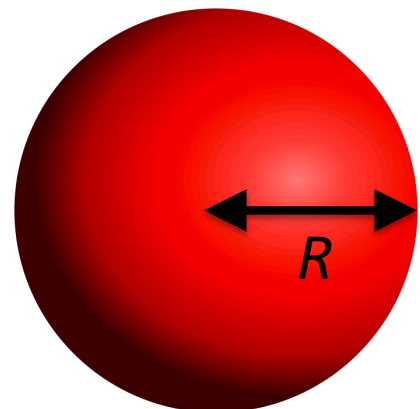
$$F_\tau(\omega, \phi, 2\tilde{\chi}) = \frac{1}{2}[e^{i\omega} + \sqrt{(1 - 2\varepsilon_{1\tau})(1 - 2\varepsilon_{2\tau})} e^{-i\phi}] \cos(2\tilde{\chi}) - \frac{i}{2}[e^{i\omega} - \sqrt{(1 - 2\varepsilon_{1\tau})(1 - 2\varepsilon_{2\tau})} e^{-i\phi}] \sin(2\tilde{\chi}),$$

Quasi-0D confinement: Unconventional optical transitions in topological- insulator nanoparticles



Topological-insulator nanoparticle: Model

- isotropic and particle-hole-symmetric version of **3D-bulk BHZ Hamiltonian + spherical hard-wall mass confinement** Imura et al., Phys. Rev. B (2012)
- relevant size scales: nanoparticle **radius R** , bulk-material **Compton length $R_0 = 2\gamma / \Delta_0$**
- previous work considered limit $R \gg R_0$



$$\mathcal{H} = \begin{pmatrix} \frac{\Delta(\mathbf{k})}{2} + V(r) & \gamma k_z & 0 & \gamma k_- \\ \gamma k_z & -\frac{\Delta(\mathbf{k})}{2} - V(r) & \gamma k_- & 0 \\ 0 & \gamma k_+ & \frac{\Delta(\mathbf{k})}{2} + V(r) & -\gamma k_z \\ \gamma k_+ & 0 & -\gamma k_z & -\frac{\Delta(\mathbf{k})}{2} - V(r) \end{pmatrix}$$



General form of TI-nanoparticle states

Gioia, Christie, UZ et al., arXiv:1906.08162

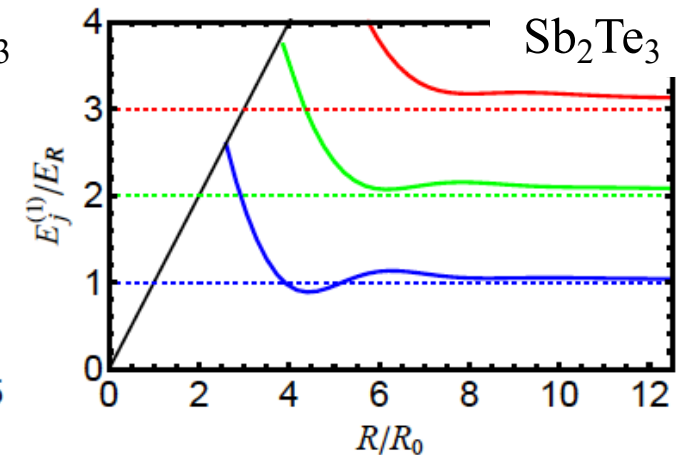
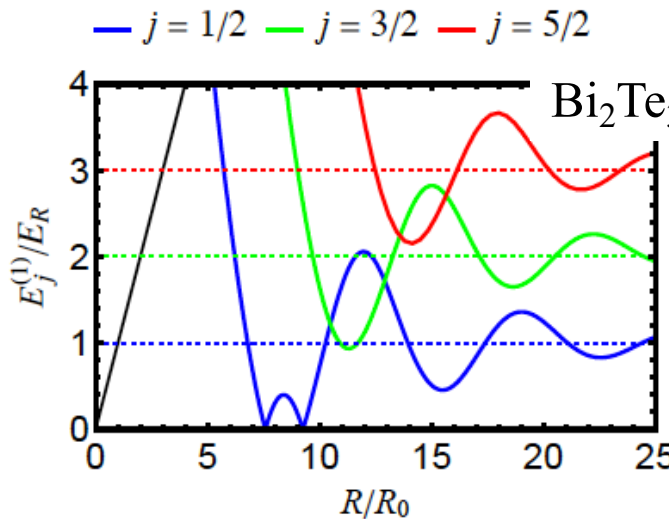
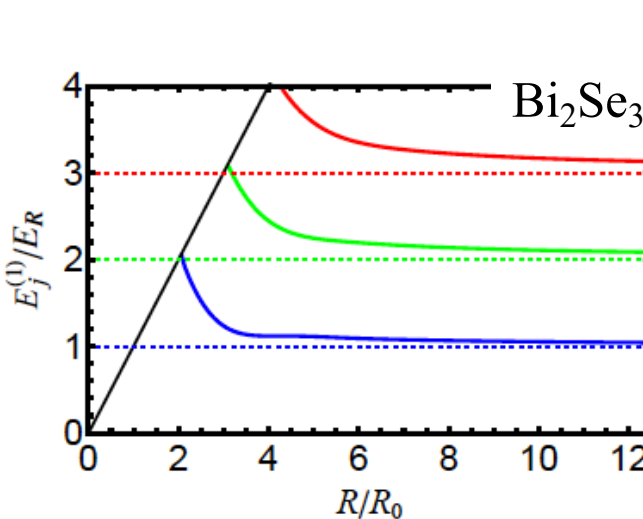
- spherical symmetry: total angular momentum j and its projection m are good quantum numbers
- ramifications of two-flavour Dirac physics
 - half-integer j (spin-1/2 spherical harmonics!)
 - two states with opposite parity exist for fixed j, m
 - intricate structure of angular and radial wave functions

$$\Psi_{jm+}^{(n)}(\mathbf{r}) = \frac{C_{j+}^{(n)}}{2} \begin{pmatrix} \sqrt{\frac{j+m}{j}} Y_{j-\frac{1}{2}}^{m-\frac{1}{2}}(\theta, \varphi) \phi_{j+\uparrow}^{(n)}(r) \\ \sqrt{\frac{j+1-m}{j+1}} Y_{j+\frac{1}{2}}^{m-\frac{1}{2}}(\theta, \varphi) \phi_{j-\uparrow}^{(n)}(r) \\ \sqrt{\frac{j-m}{j}} Y_{j-\frac{1}{2}}^{m+\frac{1}{2}}(\theta, \varphi) \phi_{j+\uparrow}^{(n)}(r) \\ -\sqrt{\frac{j+1+m}{j+1}} Y_{j+\frac{1}{2}}^{m+\frac{1}{2}}(\theta, \varphi) \phi_{j-\uparrow}^{(n)}(r) \end{pmatrix}, \quad \Psi_{jm-}^{(n)}(\mathbf{r}) = \frac{C_{j-}^{(n)}}{2} \begin{pmatrix} \sqrt{\frac{j+1-m}{j+1}} Y_{j+\frac{1}{2}}^{m-\frac{1}{2}}(\theta, \varphi) \phi_{j+\uparrow}^{(n)}(r) \\ \sqrt{\frac{j+m}{j}} Y_{j-\frac{1}{2}}^{m-\frac{1}{2}}(\theta, \varphi) \phi_{j-\uparrow}^{(n)}(r) \\ -\sqrt{\frac{j+1+m}{j+1}} Y_{j+\frac{1}{2}}^{m+\frac{1}{2}}(\theta, \varphi) \phi_{j+\uparrow}^{(n)}(r) \\ \sqrt{\frac{j-m}{j}} Y_{j-\frac{1}{2}}^{m+\frac{1}{2}}(\theta, \varphi) \phi_{j-\uparrow}^{(n)}(r) \end{pmatrix}$$



Topological-bound-state spectrum

- large- R limit: $E_j^{(1)} \rightarrow \left(j + \frac{1}{2}\right)E_R$ with $E_R = \frac{\gamma}{R}$
Imura et al., Phys. Rev. B (2012)
- significant deviations from asymptotic behaviour occur even for not-too-small nanoparticle size
- critical size R_c : no sub-gap state exists for $R < R_c$



Optical transitions: Basic theory

- selection rules and transition rates are governed by the **optical-dipole matrix elements**

$$\mathbf{d}_{n j m \kappa}^{n' j' m' \kappa'} \equiv \int d^3 r \left[\Psi_{j' m' \kappa'}^{(n')}(\mathbf{r}) \right]^\dagger \mathbf{d} \Psi_{j m \kappa}^{(n)}(\mathbf{r})$$

- both **intra-band** and **inter-band** transitions possible
 - treat both on the same footing by deriving the general envelope-function-space optical-dipole operator

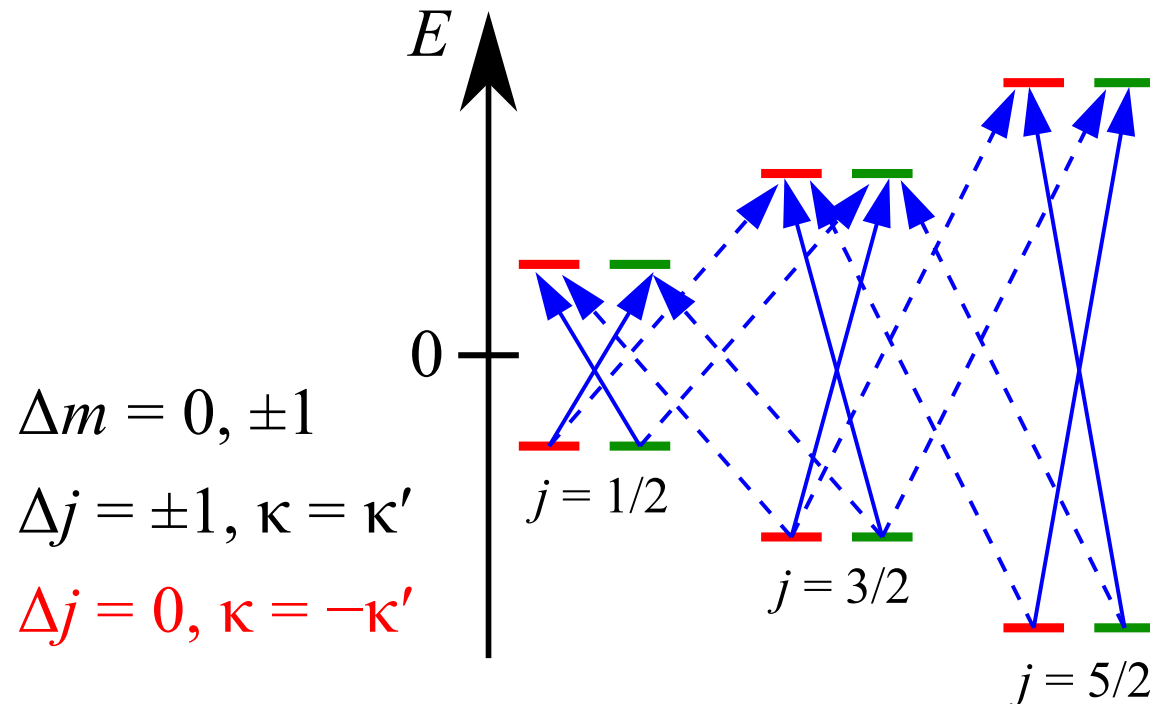
$$\mathbf{d} = e \mathbf{r} \tau_0 \otimes \boldsymbol{\sigma}_0 + \frac{e R_0}{2} \tau_y \otimes \boldsymbol{\sigma}$$

- obtain **analytical expressions** for matrix elements

Gioia, Christie, UZ, Governale, Sneyd, arXiv:1906.08162

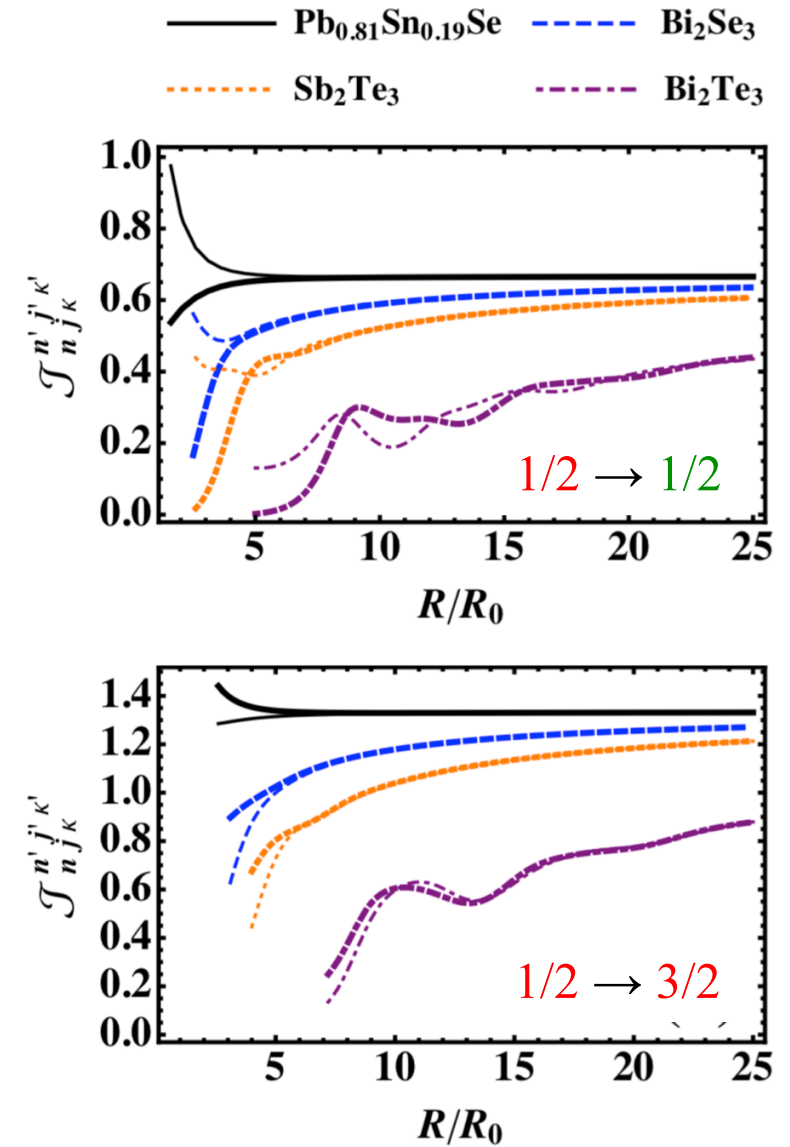


Unconventional optical-dipole transitions



$$\sum_{m=-j}^j \left| (d_x \pm id_y)_{n j m \kappa}^{n' j' m' \kappa'} \right|^2 \equiv \frac{2e^2 R^2}{3} \mathcal{T}_{n j \kappa}^{n' j' \kappa'}$$

$$\sum_{m=-j}^j \left| (d_z)_{n j m \kappa}^{n' j' m' \kappa'} \right|^2 \equiv \frac{e^2 R^2}{3} \mathcal{T}_{n j \kappa}^{n' j' \kappa'}$$



Conclusions

- used **effective (BHZ) model** of bulk topological-insulator bands to study size- quantization effects
 - (parabolic, hard-wall) **mass-confinement potential**
- quantum wells: materials dependence of **gap oscillations**, giant **Zeeman splitting** for in-plane **B**
Kotulla, UZ, New. J. Phys. **19**, 073025 (2017); Kotulla, PhD Thesis (2019)
- quantum rings: confinement-dependent **geometric phase**, **valley/spin-polarized electric conductance**
Gioia, UZ, Governale, Winkler, Phys. Rev. B **97**, 205421 (2018)
- nanoparticles: **unconventional optical transitions**
Gioia, Christie, UZ, Governale, Sneyd, arXiv:1906.08162